

# The behaviour of $^{236}\text{U}$ in the North Atlantic Ocean assessed from numerical modelling: a new evaluation of the input function into the Arctic

R. Perri  nez\*  
Dpt F  sica Aplicada I, ETSIA  
Universidad de Sevilla  
Ctra Utrera km 1  
41013-Sevilla, Spain

Byung-Il Min  
KAERI  
Daedeok-Daero 989-111  
Yuseong-Gu, Daejeon  
Republic of Korea

Kyung-Suk Suh  
KAERI  
Daedeok-Daero 989-111  
Yuseong-Gu, Daejeon  
Republic of Korea

M. Villa-Alfageme  
Dpt F  sica Aplicada II, ETSIE  
Avda Reina Mercedes s/n  
University of Sevilla  
Spain

December 27, 2017

1

## Abstract

2

3

4

5

6

7

8

9

A numerical model, previously validated with other radionuclides, was applied to simulate the dispersion of  $^{236}\text{U}$  released from European nuclear fuel reprocessing plants in the North Atlantic and Shelf Seas using a published reconstruction of Sellafield and La Hague releases. Model results are in better agreement with observations if the lowest estimation of such releases are used. This implies that approximately 40 kg of  $^{236}\text{U}$  have been discharged from Sellafield. It was found that adsorption of  $^{236}\text{U}$  on bed sediments of the shallow European Shelf Seas plays an essential role in its dispersion patterns. This contrasts strongly with the more

---

\*Corresponding author; e-mail: rperianez@us.es, phone +34 954486474, fax +34 954486436

10 conservative behavior of  $^{129}\text{I}$  in the same area. This has two important implications  
11 in the use of  $^{236}\text{U}$  as oceanographic tracer; i) special care must be taken in coastal  
12 areas, as sediments might act as sinks and sources of  $^{236}\text{U}$ ; ii) the annual input  
13 function of  $^{236}\text{U}$  into the Arctic is not directly controlled by the annual discharges  
14 from Sellafield and La Hague, since sediments from the Irish, Celtic and North Sea  
15 modulate and smooth the signal. Only 52% of the total releases enter into the Arctic  
16 Ocean.

17 *Keywords:* Lagrangian model; North Atlantic; 236-uranium; sediments; water tracer;  
18 Nuclear Fuel Reprocessing Plants

## 19 **1 Introduction**

20 The characterization of the Arctic water masses has become fundamental in the late years,  
21 e.g., to understand how climate change would affect circulation patterns in the region.  
22 New data and updated models are of primary importance for tracing transport pathways  
23 and features of the Arctic water masses. Anthropogenic radionuclides, such as  $^{137}\text{Cs}$ ,  $^3\text{H}$ ,  
24  $^{99}\text{Tc}$  and  $^{129}\text{I}$ , are being used as transient tracers of oceanographic processes.

25  $^{236}\text{U}$  has been presented in the last years as a powerful new water mass tracer in  
26 oceanography, especially in the Atlantic Ocean and Arctic Ocean. It is almost entirely,  
27 but not exclusively, of anthropogenic origin. A total amount of 35 kg of mobile  $^{236}\text{U}$  is  
28 estimated to come from natural sources, atmospheric nuclear weapons tests contributed  
29 to the total inventory with about 900 kg (Sakaguchi et al., 2009)). Finally, the Nuclear  
30 Fuel Reprocessing Plants (NFRP) of Sellafield, Springfields and La Hague have carried  
31 out significant liquid discharges to the sea.  $^{236}\text{U}$  contribution from these sources has been  
32 estimated to be about 95 kg (Christl et al., 2015a). However, these estimations still need  
33 to be narrowed down. In order to use  $^{236}\text{U}$  as a robust oceanographic tracer, it is essential

34 to quantify accurately the contribution of the different sources and to better define its  
35 geochemical behavior. A full three-dimensional Lagrangian model which simulates the  
36 dispersion of  $^{236}\text{U}$  through the North Atlantic (NA) has been used to evaluate the annual  
37 discharges and the total amount of  $^{236}\text{U}$  released in the NA from the NFRP. Further-  
38 more, using the model it is possible to investigate, for the first time, the water/sediment  
39 interactions of  $^{236}\text{U}$ .

40 The model was previously applied to study the dispersion of  $^{129}\text{I}$  and  $^{137}\text{Cs}$  released  
41 from the European NFRP (Villa et al., 2015; Periañez et al., 2017, respectively) and  
42 its results were compared with measurements in both water and sediments. These are  
43 geochemically well-known radionuclides, with well-known discharges from the NFRP. It  
44 allowed us to evaluate the performances of the model. The next step has been to imple-  
45 ment the model to improve our knowledge of  $^{236}\text{U}$ .

46 The model is described in detail in references cited above and, consequently, only  
47 a brief overview is provided in section 2. Model results are presented in section 3. A  
48 reconstruction of Sellafield releases was required to run the model. Results show that  
49 the lowest estimations of such releases should be used to have a better agreement with  
50 observations. This is described in section 3.1. An investigation on  $^{236}\text{U}/^{129}\text{I}$  ratios is  
51 presented in section 3.2, where it is shown that they must be carefully analyzed when  
52 used as water tracers, since  $^{129}\text{I}$  is significantly more conservative than  $^{236}\text{U}$ . Finally, a  
53 reconstruction of the  $^{236}\text{U}$  input function into the Arctic Ocean is presented in section  
54 3.3.

## 55 **2 Model description**

56 The model is a full three-dimensional Lagrangian dispersion model in which a radionuclide  
57 release is simulated by a number of particles, each of them equivalent to a number of units

58 (atoms in the present application). The three-dimensional path followed by each particle  
59 is computed, turbulent diffusion being modelled as a three-dimensional random walk  
60 process. A constant typical value of  $1.0 \times 10^{-3} \text{ m}^2/\text{s}$  (Elliott et al., 2001) has been used  
61 for the vertical diffusivity. In a previous work on  $^{129}\text{I}$  dispersion, it has been tested that  
62 model results are little sensitive to this parameter (Villa et al. 2015). The Smagorinsky's  
63 scheme (Cushman-Roisin and Beckers, 2011) has been adopted to describe the horizontal  
64 diffusivity.

65 The number of particles per water volume unit is computed to obtain radionuclide  
66 concentrations over the domain at the desired times and depths.

67 Interactions between the dissolved phase and solid phases (suspended matter and bed  
68 sediments) are described through a dynamic approach. Thus, uptake/release of radionu-  
69 clides is considered to be described by a reversible reaction. This reaction is described by  
70 kinetic rates  $k_1$  and  $k_2$  as in previous works (Periáñez, 2008; 2012; Periáñez et al., 2013,  
71 among many others). A stochastic method was developed to solve the equations describ-  
72 ing these processes. Technical details may be consulted elsewhere (Periáñez and Elliott,  
73 2002; Periáñez and Caravaca, 2010; Villa et al., 2015; Periáñez et al., 2016). This method  
74 for describing water/sediment interactions has been used by other researches (Kobayashi  
75 et al., 2007; Min et al., 2013; Zhang and Battista, 2008) and successfully applied in model  
76 intercomparison exercises (Periáñez et al., 2015).

77 The considered domain in the north Atlantic extends from  $50^\circ \text{ W}$  to  $25^\circ \text{ E}$  in longitude  
78 and from  $45.1^\circ \text{ N}$  to  $75.1^\circ \text{ N}$  in latitude (Fig. 1). Water circulation for the period of interest  
79 is required since currents are the main vector for the transport of tracers through advection  
80 processes. It has been obtained from JAMSTEC (Japan Agency for Marine-Earth Science  
81 and Technology) global ocean model. It is OFES (Ocean global circulation model For the  
82 Earth Simulator)<sup>1</sup>. A comparison of model performance with data in several regions of

---

<sup>1</sup>[http://www.jamstec.go.jp/esc/research/AtmOcn/product/ofes.html#cite\\_note-1](http://www.jamstec.go.jp/esc/research/AtmOcn/product/ofes.html#cite_note-1)

83 the global ocean (including the North Atlantic) may be seen in Masumoto et al., (2004).  
84 Horizontal resolution is  $0.1^\circ$  and there are 54 vertical levels, with increasing thickness  
85 from the surface towards the sea bottom. Monthly mean circulation has been used. As  
86 an example, surface circulation for January 2008 is shown in Fig. 1.

87 The model has already been successfully applied to simulate the dispersion of historical  
88 radionuclide releases from Sellafield and La Hague nuclear fuel reprocessing plant (Villa  
89 et al. 2015; Perrinez et al., 2016). In particular releases of  $^{129}\text{I}$ , considering it as a  
90 perfectly conservative tracer, thus remaining in solution (Villa et al., 2015), and releases  
91 of  $^{137}\text{Cs}$  (Perrinez et al., 2016). In this last case exchanges of radionuclides between  
92 water, suspended matter and bed sediments were considered. Computed and measured  
93  $^{137}\text{Cs}$  distributions in water and bed sediments at several areas of the European Shelf  
94 and at different times were compared. Model results were in reasonable agreement with  
95 observations (Perrinez et al., 2016).

96 Historical releases of  $^{129}\text{I}$  and  $^{236}\text{U}$  from Sellafield and La Hague for the period of  
97 interest (1952-2013, which is the time extent of the simulations) are presented in Fig. 2.  
98 In the case of  $^{129}\text{I}$ , release data is obtained from Lpez-Gutirrez et al. (2004); Sellafield  
99 (2014); Areva (2014). In the case of  $^{236}\text{U}$  information is more limited. La Hague facility  
100 has provided these releases with a few gaps. The full sequence has been reconstructed by  
101 Christl et al. (2015a). The authors have also reconstructed  $^{236}\text{U}$  releases from Sellafield  
102 based on total uranium discharges. Three different reconstructions were carried out and  
103 the mean value and standard error were provided in Christl et al. (2015a). Such mean  
104 value is the red line in Fig. 2. Upper and lower limits, taken as the uncertainty of the  
105 mean, are indicated by the dashed black lines. The smaller releases from Springfield  
106 reprocessing plant (UK) are also given in Christl et al. (2015a) and they are included in  
107 simulations described in this paper.

## 108 **3 Results**

109 The model was initially applied to  $^{129}\text{I}$  and compared with measurements (other than  
110 those already used in Villa et al., 2015). These are mean concentration in North Sea water  
111 in 2005 (Michel et al., 2012) and 2009 (Christl et al., 2015b); as well as a distribution  
112 map over this area in Christl et al. (2015b). Then the model was applied to  $^{236}\text{U}$  and  
113 compared with mean concentration of this radionuclide in the North Sea in 2009 and  
114 its spatial distribution here (Christl et al., 2015b). Calculated and measured (Christl et  
115 al., 2015b)  $^{129}\text{I}/^{236}\text{U}$  ratios were also compared. Subsequently the model was applied to  
116 evaluate the new  $^{236}\text{U}$  input function into the Arctic.

### 117 **3.1 $^{236}\text{U}$ and $^{129}\text{I}$ dispersion**

118 Background concentrations of  $^{236}\text{U}$  and  $^{129}\text{I}$  due to nuclear weapon test fallout should  
119 be considered in order to compare model results and measurements. According to the  
120 estimation in Christl et al. (2015a), fallout background in the North Sea in 2009 (year  
121 and area where measurements are available), is about  $10^7$  at/kg for  $^{236}\text{U}$  and about ten  
122 times smaller for  $^{129}\text{I}$ . These uniform background values have been directly added to the  
123 calculated concentrations associated to the reprocessing plants.

124 Model simulations for  $^{129}\text{I}$ , considering it as a perfectly conservative radionuclide,  
125 were described in Villa et al. (2015). To compare its behavior with the results from  $^{236}\text{U}$ ,  
126 additional results from such simulations are presented in this work. Thus, a comparison  
127 of the calculated and measured (Christl et al., 2015b) distribution in surface water of the  
128 North Sea in 2009 is presented in Fig. 3. The calculated distribution of  $^{129}\text{I}$  is in general  
129 agreement with the measured one. A plot of measured vs. calculated concentrations can  
130 be seen in Fig. 4. Due to the Lagrangian nature of the model, not all the grid cells in  
131 which measurements are available were occupied by particles. Thus, not all observations

132 in Christl et al. (2015b) can be plotted. It is more adequate, in Lagrangian models, to look  
133 at general trends and averaged values over relatively larger regions than to measurements  
134 at given points. This is confirmed in the top panel of Fig. 5 where the temporal evolution  
135 of the calculated mean  $^{129}\text{I}$  concentration over the surface water of the North Sea is shown.  
136 The calculated mean is obtained as the total  $^{129}\text{I}$  content in the North Sea divided by  
137 the total water volume in the sea. Measured arithmetic mean concentrations, together  
138 with their  $1\sigma$  standard deviations, in 2005 (Michel et al., 2012) and 2009 (Christl et al.,  
139 2015b) are also drawn. The calculated trend indicates an increase in concentrations in the  
140 beginning of the 1990s, due to the increase in La Hague releases (Fig. 2), and measured  
141 mean levels are well determined by the model. Although the model tends to overestimate  
142 measured concentrations when compared point by point (Fig. 4), general distribution  
143 patterns and mean values are in reasonable agreement with observations.

144 The model, that works satisfactorily in the case of  $^{129}\text{I}$ , has been applied to  $^{236}\text{U}$ . No  
145 calibration for this radionuclide has been carried out and initially the only change is the  
146 magnitude of the  $^{236}\text{U}$  releases from Sellafield, La Hague and Springfield.

147 Calculated and measured mean concentrations in surface water of the North Sea are  
148 presented in Fig. 5 (central panel). The blue and red lines correspond, respectively, to  
149 simulations made with the mean value and the lower limit of the Sellafield releases (red  
150 line and lower black dashed lines in the bottom panel of Fig. 2). It is clear that, even with  
151 the lower estimation of the discharge, the mean  $^{236}\text{U}$  concentration dissolved in the surface  
152 water of the North Sea in 2009 shown in the figure ( $75 \times 10^6$  at  $\text{kg}^{-1}$ ) is overestimated  
153 by the present parameterization of the model.

154 The equilibrium distribution coefficient ( $k_d$ ) of natural uranium, is of the same order  
155 of magnitude as that of Cs (IAEA, 2004). And since there are not indications that  
156  $^{236}\text{U}$  and natural uranium behave differently in the ocean (Casacuberta et al., 2016 and

157 references therein), a fraction of the released  $^{236}\text{U}$  might be removed by the sediments  
158 of the shallow shelf seas, as it actually happens for  $^{137}\text{Cs}$ . An additional simulation was  
159 carried out to test this hypothesis. Model parameters required to describe water/sediment  
160 interactions are described in several references (Periáñez, 2005; Periáñez, 2008; Periáñez  
161 et al., 2016). Again any model calibration has not been carried out. The model runs  
162 with the same parameters as for  $^{137}\text{Cs}$  (Periáñez et al., 2016) except the different releases  
163 from the reprocessing plants and the value of the radionuclide  $k_d$ . Although the model  
164 describes radionuclide exchanges between the dissolved and solid phases in a dynamic  
165 way, the equilibrium  $k_d$  is used to derive the adsorption kinetic rate as explained in detail  
166 in Periáñez et al. (2016) and references therein. The value recommended by IAEA (2004)  
167 for coastal waters has been used for the U  $k_d$ :  $1.0 \times 10^3$  (dimensionless). A summary  
168 of parameters required by the model to describe water/sediment interactions is given in  
169 Table 1. These parameters have been considered uniform over the whole model domain.  
170 This is an approximation, due to the lack of information about their variability over such  
171 a large region, which obviously will lead to some unavoidable errors in predictions. In  
172 spite of this, the general behaviour of  $^{236}\text{U}$  in sediments should be given by the model,  
173 since it was successfully applied to describe patterns of  $^{137}\text{Cs}$  in sediments with the same  
174 parameter set (except the  $k_d$ ).

175 The result of this new simulation is presented in the central panel of Fig. 5 (black  
176 line). The “kinetics” simulation corresponds to the lower limit of Sellafield releases and  
177 includes interactions of the  $^{236}\text{U}$  between water and sediments. The mean  $^{236}\text{U}$  dissolved  
178 levels in the North Sea inferred from this new simulation is in better agreement with the  
179 experimental values.

180 Additionally, the calculated inventories of  $^{236}\text{U}$  over the model domain in bed sediments  
181 in 2013 is presented in Fig. 6. It is shown that  $^{236}\text{U}$  is mainly absorbed in the sediments of



parameter description	value
sediment mixing depth	$L = 0.05$ m
particle density	$\rho = 2600$ kg/m <sup>3</sup>
correction factor	$\phi = 0.1$
sediment porosity	$p = 0.6$
desorption kinetic coefficient	$k_2 = 1.16 \times 10^{-5}$ s <sup>-1</sup>
U distribution coefficient	$k_d = 1.0 \times 10^3$
particle radius	$1.0 \times 10^{-6}$ m

Table 1: Summary of model parameters involved in water/sediment interaction description. Parameter  $\phi$  is a correction factor which takes into account that not all the sediment particle surface is available to adsorb radionuclides since may be partially hidden by other particles.

182 the shallow areas; this way relatively high <sup>236</sup>U concentrations are present in the Celtic Sea  
183 sediments of the continental shelf, and in the Irish Sea and English Channel (where releases  
184 from Sellafield and La Hague occur, respectively). Releases from Sellafield are higher than  
185 releases from La Hague since the 1990s (Fig. 2). Thus, inventories in the Irish Sea reach  
186 the highest values. Furthermore, releases from both plants are transported by currents to  
187 the North Sea, thus sediments in this shallow sea also show significant inventories. Values  
188 in the Celtic Sea are in the order of  $10^{11} - 10^{12}$  at/m<sup>2</sup>. The results are in agreement with  
189 the <sup>236</sup>U concentrations measured in two sediment cores collected in the area in 2015,  
190 which ranged from 10 to  $20 \times 10^{11}$  at/m<sup>2</sup> (Villa-Alfageme et al., unpublished). Calculated  
191 and measured values were higher than <sup>236</sup>U concentrations measured in sediments from  
192 the North Atlantic Porcupine Abyssal Plain (PAP) site -4500 m depth, 49°00' N, 16°30'  
193 W- (Villa-Alfageme et al. 2017). The reasons are i) <sup>236</sup>U water concentration at the  
194 PAP site is significantly lower than at the North Sea since the contribution is mostly due  
195 to fall-out ii) PAP site is a deep-sea area, where particle concentrations and downward  
196 flux are significantly lower than at the European Shelf Seas. Furthermore, modelled  
197 and measured inventories at the Celtic Sea are an order of magnitude higher than the

198 inventories measured at the Japan Sea (Sakaguchi et al., 2012), which is an area not  
199 affected by NFRP discharges.

200 The calculated distribution of  $^{236}\text{U}$  in surface water of the North Sea in 2009 is pre-  
201 sented in Fig. 7 (top row), together with the map obtained after interpolation of measure-  
202 ments, which has been taken from Christl et al. (2015b). Calculated levels are in relative  
203 good agreement with the measured ones. However, the model largely overestimated con-  
204 centrations when the medium value of the Sellafield release was used and water/sediment  
205 interactions were neglected (maps not shown). A comparison of measured vs. calculated  
206 concentrations in this simulation is presented in Fig. 4. The same comments as for  $^{129}\text{I}$   
207 can be done.

208 Our results show that a) the present Sellafield releases are probably biased towards  
209 the lower estimations given by Christl et al. (2015a) and b) adsorption of  $^{236}\text{U}$  on bed  
210 sediments of the shallow European Shelf Seas plays an essential role in its dispersion  
211 patterns in these areas. This points out that the geochemical behaviour of  $^{236}\text{U}$  differs  
212 from that of  $^{129}\text{I}$  in coastal areas and the continental shelf, and they might not be as  
213 similar as previously predicted for open sea water (Christl et al., 2013; 2015a; 2015b).  
214 While  $^{129}\text{I}$  may be considered completely conservative, this is not the case of  $^{236}\text{U}$  (IAEA,  
215 2004). The implication of this result is that the transferences of  $^{236}\text{U}$  between water and  
216 sediments should be considered for an accurate simulation of dispersion in shallow waters.  
217 Consequently, a further analysis of the  $^{129}\text{I}/^{236}\text{U}$  ratios in coastal areas must be done when  
218 this ratio is used as an complementary tracer of water masses (Casacuberta et al., 2016).

### 219 **3.2 $^{129}\text{I}/^{236}\text{U}$ ratios**

220 Mean calculated and measured  $^{129}\text{I}/^{236}\text{U}$  ratios in the surface water of the North Sea in  
221 2009 are presented in the bottom panel of Fig. 5. In both cases (model and measurements)

222 they are obtained similarly as a ratio between the mean concentrations (either from the  
223 model or measurements). The results are in good agreement within the uncertainty of the  
224 experimental values. This  $^{129}\text{I}/^{236}\text{U}$  function has been also reconstructed in Christl et al.  
225 (2015a) using a single box model of the North Sea and assuming that  $^{236}\text{U}$  is a perfectly  
226 conservative tracer (figure 10 in their paper). Such function shows a clear monotonic  
227 increase from 1990 to 2010. The present model, however, predicts quite steady values for  
228 the ratio since approximately year 2000.

229 Calculated and measured  $^{129}\text{I}/^{236}\text{U}$  ratios, again in surface water sampled in 2009, are  
230 shown in Fig. 7 (bottom row), modelled and experimental values are in good agreement.  
231 The dark blue color in the calculation map implies background levels for the ratio. Waters  
232 coming from Sellafield and La Hague clearly show different values for the ratios, which  
233 are higher for waters entering the North Sea from the English Channel. Indeed,  $^{129}\text{I}/^{236}\text{U}$   
234 ratios in the direct releases made from Sellafield and La Hague are presented independently  
235 in Fig. 8. Ratios in discharges from La Hague are above  $10^3$  since 2009, while in Sellafield  
236 releases it is below  $10^2$ .

237 It is noteworthy to mention that the modelled ratios calculated for both La Hague and  
238 Sellafield water entering the North Sea branches are above the ratio values from the direct  
239 discharges; this is even more apparent in the case of Sellafield, where modelled ratios are  
240 approximately an order of magnitude above those of the direct discharges. Note that the  
241 comparison with the measured data is difficult since, this Sellafield branch is essentially  
242 missed in the measurement map since there are not sampling points near the shore as  
243 required. The high ratios in relation to direct discharges are explained according to the  
244 removal of  $^{236}\text{U}$  in bed sediments; and they are even higher in Sellafield because waters  
245 travelling from Sellafield cover a larger distance than waters coming from La Hague, thus  
246 a larger amount of  $^{236}\text{U}$  is lost in the sediments. Consequently, the differences in the ratios

247 between the water branch entering the North Sea and the releases are higher in the case  
248 of Sellafield than in La Hague.

249 These results point out that  $^{129}\text{I}/^{236}\text{U}$  ratios must be carefully analyzed when used as  
250 water tracers, since I is significantly more conservative than U (as actually indicated  
251 by the  $k_d$  recommended for these elements by IAEA [2004]).

### 252 **3.3 $^{236}\text{U}$ input function into the Arctic**

253 The input function of  $^{236}\text{U}$  into the Arctic Ocean from the Norwegian Coastal Current  
254 (NCC) has been reconstructed with the model. Thus, the annual input,  $I$ , is calculated  
255 as  $I = F \cdot C$ , where  $C$  is the mean concentration of  $^{236}\text{U}$  in the NCC (which is the vector  
256 transporting material from the European Shelf into the Arctic) and  $F$  is the Norwegian  
257 Current water flow.  $F$  has been calculated from the currents provided by JAMSTEC ocean  
258 model used to drive the present dispersion model. Such flow results  $F = (1.5 \pm 0.3) \times 10^7$   
259  $\text{m}^3/\text{s}$  at  $70^\circ$  N latitude (where  $\pm 0.3$  is the standard deviation from 60 monthly values).  
260 The resulting modelled  $^{236}\text{U}$  input signal into the Arctic is given in Fig. 9, together with  
261 the signal expected from the direct releases from the different NFRP (shown in the same  
262 plot). These curves (given in  $\text{kg year}^{-1}$ ) are integrated to obtain the total amount of  $^{236}\text{U}$ .  
263 Thus, the total  $^{236}\text{U}$  input released from La Hague is 24.03 kg and from Sellafield it is  
264 40.47 kg (note that we are using the lower value of the estimation of Christl et al., 2015a).  
265 Sellafield plus La Hague input (SF+LH in Fig.9) is 64.50 kg, and Springfield releases add  
266 8.93 kg. Finally, we calculated that the total modelled input into the Arctic (given by  
267 the integral of the black curve in Fig. 9), that is  $38 \pm 8$  kg. This amount corresponds  
268 to only  $52 \pm 11$  % of the total  $^{236}\text{U}$  73.43 kg released from Sellafield, Springfield and La  
269 Hague. The missing  $^{236}\text{U}$  was stored in bed sediments, mostly in shallow waters, and  
270 retained in areas like the Baltic Sea, which has a mean residence time of about 10-30

271 years (Leppäranta and Myberg, 2009).

272 An interesting point is that the modelled signal into the Arctic does not reproduce  
273 the increases and decreases of the discharges of  $^{236}\text{U}$  from Sellafield and La Hague into  
274 the ocean. There is an abrupt increase in the discharges from 1970 to approximately  
275 1985. A secondary maximum is found in 1995 and afterwards, there is a reduction of  
276 Sellafield and La Hague  $^{236}\text{U}$  discharges until the signal reached a rather steady value  
277 slightly lower than 1.5 kg/year. In the model, there is a monotonous increase in the  
278 input function from 1970 to approximately year 1990. After that year, the modelled  
279 input function remains constant around a value of 1.5 kg/year. Before the year 2000 the  
280 modelled signal was significantly lower than the direct discharges, this trend is reversed  
281 in 2000, where the modelled signal remains constant, but slightly over 1.5 kg/year and  
282 the direct discharges. The reason for this evolution is that initially the sediments were  
283 acting mainly as sinks of  $^{236}\text{U}$ , until equilibrium between the two compartments water  
284 and sediments is reached, and sediment act both as sinks and sources.

285 In terms of the  $^{236}\text{U}$  signal into the Arctic, our results have two implications. First,  
286 as predicted in the previous section, the amount of  $^{236}\text{U}$  entering into the Arctic is lower  
287 than the amount of  $^{236}\text{U}$  directly released by the NFRP; and second, the interaction with  
288 sediment in the European Shelf shape the signal into the Arctic, and smooth abrupt  
289 changes of the direct discharges from NFRP.

## 290 4 Conclusions

291 A Lagrangian three-dimensional dispersion model, previously tested for  $^{129}\text{I}$  and  $^{137}\text{Cs}$ ,  
292 has been applied to simulate the behaviour of  $^{236}\text{U}$  released from European nuclear fuel  
293 reprocessing facilities in the North Atlantic Ocean.

294 The present model indicates that the actual Sellafield releases seem to be in agreement

295 with the lower estimations of Christl et al. (2015a). This implies a total release of about  
296 40 kg of  $^{236}\text{U}$  from this facility. Also, adsorption of  $^{236}\text{U}$  on bed sediments of the shallow  
297 European Shelf Seas seem to play an essential role in its dispersion patterns in these areas.  
298 Consequently, part of the released  $^{236}\text{U}$  is trapped in sediments. . This figure implies a  
299 total mass of  $38 \pm 8$  kg of  $^{236}\text{U}$  into the Arctic from the three NFRP. The input function  
300 has also been reconstructed.

301 It has been found that the geochemical behaviour of  $^{129}\text{I}$  and  $^{236}\text{U}$  is not as similar as  
302 stated in other previous works. In the first case, adsorption in sediments can be neglected,  
303 but it has to be considered for a proper dispersion simulation in the case of  $^{236}\text{U}$ . Thus,  
304 special care should be taken when ratios between these isotopes are used to trace waters  
305 in shallow seas.

## 306 **Acknowledgements**

307 Work partially supported by project FIS2015-69673-P of the Spanish Ministerio de  
308 Economía y Competitividad: Resolución de problemas ambientales marinos y terrestre  
309 clave mediante nuevos desarrollos en Espectrometría de Masas con Acelerador de Baja  
310 Energía (LEAMS) en el Centro Nacional de Aceleradores (CNA). Also supported by  
311 the National Research Foundation of Korea (NRF) and funded by the Korea government  
312 (MSIP: NRF-2017M2A8A4015253, NRF-2015M2A2B2034282). The authors are indebted  
313 to Marcus Christl and Nuria Casacuberta (Laboratory of Ion Beam Physics, Zurich) for  
314 kindly providing their estimations on  $^{236}\text{U}$  releases from Sellafield.

## 315 **5 References**

316 Areva, 2014. [http://www.areva.com/EN/operations-2315/cumulative-release-results-](http://www.areva.com/EN/operations-2315/cumulative-release-results-report-for-the-areva-la-hague-plant.html)  
317 [report-for-the-areva-la-hague-plant.html](http://www.areva.com/EN/operations-2315/cumulative-release-results-report-for-the-areva-la-hague-plant.html)

318 Casacuberta, N., Masqué, P., Henderson, G., Rutgers van-der-Loeff, M., Bauch, D.,  
319 Vockenhuber, C., Daraoui, A., Walther, C., Synal, H.A., Christl, M., 2016. First  
320  $^{236}\text{U}$  data from the Arctic Ocean and use of  $^{236}\text{U}/^{238}\text{U}$  and  $^{129}\text{I}/^{236}\text{U}$  as a new dual  
321 tracer. *Earth and Planetary Science Letters* 440, 127-134.

322 Christl, M., Lachner, J., Vockenhuber, C., Goroncy, I., Herrmann, J., Synal, H.A.,  
323 2013. First data of uranium-236 in the North Sea. *Nuclear Instruments and Methods*  
324 *in Physics Research B* 294, 530-536.

325 Christl, M., Casacuberta, N., Vockenhuber, C., Elsässer, C., Bailly du Bois, P.,  
326 Herrmann, J., Synal, H.A., 2015a. Reconstruction of the  $^{236}\text{U}$  input function for the  
327 Northeast Atlantic Ocean: Implications for  $^{129}\text{I}/^{236}\text{U}$  and  $^{236}\text{U}/^{238}\text{U}$ -based tracer  
328 ages. *Journal of Geophysical Research: Oceans* 10.1002/2015JC011116.

329 Christl, M., Casacuberta, N., Lachner, J., Maxeiner, S., Vockenhuber, C., Synal,  
330 H.A., Goroncy, I., Herrmann, J., Daraoui, A., Walther, C., Michel, R., 2015b. Status  
331 of  $^{236}\text{U}$  analysis at ETH Zurich and the distribution of  $^{236}\text{U}$  and  $^{129}\text{I}$  in the North  
332 Sea in 2009. *Nuclear Instruments and Methods in Physics Research B* 361,510-516.

333 Cushman-Roisin, B., Beckers, J.M., 2011. *Introduction to Geophysical Fluid Dy-*  
334 *namics*. Elsevier.

335 Elliott, A.J., Wilkins, B.T., Mansfield, P., 2001. On the disposal of contaminated  
336 milk in coastal waters. *Marine Pollution Bulletin* 42, 927-934.

337 IAEA, 2004. Sediment distribution coefficients and concentration factors for biota  
338 in the marine environment. *Technical Reports Series* 422, Vienna.

339 Kobayashi, T., Otosaka, S., Togawa, O., Hayashi, K., 2007. Development of a  
340 nonconservative radionuclides dispersion model in the ocean and its application

341 to surface cesium-137 dispersion in the Irish Sea. *Journal of Nuclear Science and*  
342 *Technology* 44(2), 238-247.

343 Leppäranta, M., Myberg, K., 2009. *Physical Oceanography of the Baltic Sea.*  
344 Springer, Berlin.

345 López-Gutiérrez, J.M., García-León, M., Schnabel, Ch., Suter, M., Synal, H.A.,  
346 Szidat, S., García-Tenorio, R., 2004. Relative influence of  $^{129}\text{I}$  sources in a sediment  
347 core from the Kattegat area. *Science of the Total Environment* 323, 195-210.

348 Masumoto, Y., Sasaki, H., Kagimoto, T., Komori, N., Ishida, A., Sasai, Y., Miyama,  
349 T., Motoi, T., Mitsudera, H., Takahashi, K., Sakuma, H., Yagamata, T., 2004. A  
350 fifty-year eddy-resolving simulation of the World Ocean - preliminary outcomes of  
351 OFES (OGCM for the Earth Simulator). *Journal of the Earth Simulator* 1, 36-56.

352 Michel, R., Daraoui, A., Gorny, M., Jakob, D., Sachse, R., Tosch, L., Nies, H.,  
353 Goroncy, I., Herrmann, J., Synal, H.A., Stocker, M., Alfimov, V., 2012. Iodine-129  
354 and iodine-127 in European seawaters and in precipitation from Northern Germany.  
355 *Science of the Total Environment* 419, 151-169.

356 Min, B.I., Periañez, R., In-Gyu Kim, Kyung-Suk Suh, 2013. Marine dispersion  
357 assessment of  $^{137}\text{Cs}$  released from the Fukushima nuclear accident. *Marine Pollution*  
358 *Bulletin* 72, 22-33.

359 Periañez, R., 2005. *Modelling the Dispersion of Radionuclides in the Marine Envi-*  
360 *ronment.* Springer-Verlag, Heidelberg.

361 Periañez, R., 2008. A modelling study on  $^{137}\text{Cs}$  and  $^{239,240}\text{Pu}$  behaviour in the  
362 Alborán Sea, western Mediterranean. *Journal of Environmental Radioactivity* 99,  
363 694-715.



364 Periañez, R., 2012. Modelling the environmental behavior of pollutants in Algeciras  
365 Bay (south Spain). *Marine Pollution Bulletin* 64, 221-232.

366 Periañez, R., Elliott, A.J., 2002. A particle tracking method for simulating the  
367 dispersion of non conservative radionuclides in coastal waters. *Journal of Environ-  
368 mental Radioactivity* 58, 13-33.

369 Periañez, R., Caravaca, F., 2010. A set of rapid-response models for pollutant  
370 dispersion assessments in southern Spain coastal waters. *Marine Pollution Bulletin*  
371 60, 1412-1422.

372 Periañez, R., Casas-Ruiz, M., Bolívar, J.P., 2013. Tidal circulation, sediment and  
373 pollutant transport in Cádiz Bay (SW Spain): a modelling study. *Ocean Engineer-  
374 ing* 69, 60-69.

375 Periañez, R., Brovchenko, I., Duffa, C., Jung, K.T., Kobayashi, T., Lamego, F.,  
376 Maderich, V., Min, B.I., Nies, H., Osvath, I., Psaltaki, M., Suh, K.S., 2015. A new  
377 comparison of marine dispersion model performances for Fukushima Dai-ichi releases  
378 in the frame of IAEA MODARIA program. *Journal of Environmental Radioactivity*  
379 150, 247-269.

380 Periañez, R., Kyung-Suk Suh, Byung-Il Min, 2016. The behaviour of  $^{137}\text{Cs}$  in the  
381 North Atlantic Ocean assessed from numerical modelling: releases from nuclear fuel  
382 reprocessing factories, redissolution from contaminated sediments and leakage from  
383 dumped nuclear wastes. *Marine Pollution Bulletin* 113, 343-361.

384 Sakaguchi, A., Kawai, K., Steier, P., Quinto, F., Mino, M., Tomita, J., Hosh, i, M.,  
385 Whitehead, N., Yamamoto, M., 2009. First results on  $^{236}\text{U}$  levels in global fallout.  
386 *Science of the Total Environment* 407,4238-4242.

387 Sakaguchi, A., Kadokura, A., Steier, P., Takahashi, Y., 2012. Uranium-236 as a  
388 new oceanic tracer: A first depth profile in the Japan Sea and comparison with  
389 caesium-137. *Earth and Planetary Science Letters* 333-334, 165-170.

390 Sellafield, 2014. [http://sustainability.sellafieldsites.com/environment/environment-](http://sustainability.sellafieldsites.com/environment/environment-page/annual-discharge-monitoring-reports/)  
391 [page/annual-discharge-monitoring-reports/](http://sustainability.sellafieldsites.com/environment/environment-page/annual-discharge-monitoring-reports/)

392 Villa, M., López-Gutiérrez, J.M., Suh, K.S., Min, B.I., Periañez, R., 2015. The  
393 behaviour of  $^{129}\text{I}$  released from nuclear fuel reprocessing factories in the North At-  
394 lantic Ocean and transport to the Arctic assessed from numerical modelling. *Marine*  
395 *Pollution Bulletin* 90, 15-24.

396 Villa-Alfageme, M., Chamizo, E., Santos-Arevalo, F.J., López-Gutierrez, J.M., Gómez-  
397 Martínez, I., Hurtado, S., in press. First comprehensive analysis of  $^{236}\text{U}$  in a marine  
398 core in the North Atlantic Ocean. *Journal of Environmental Radioactivity*.

399 Zhang, Y., Battista, A.M., 2008. SELFE: A semi-implicit Eulerian-Lagrangian  
400 finite-element model for cross-scale ocean circulation. *Ocean Modelling* 21(3-4),  
401 71-96.

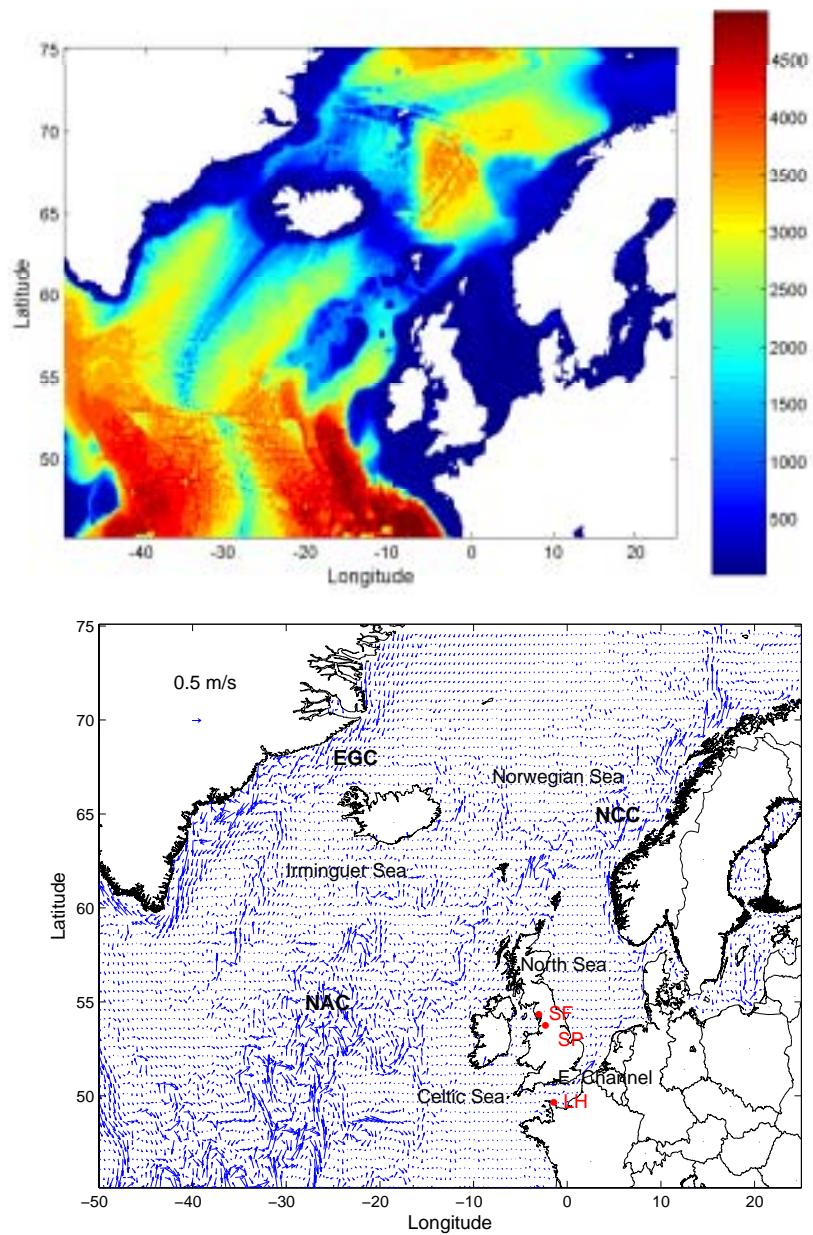


Figure 1: Top: Model domain, water depths in m. Bottom: Surface currents calculated by JAMSTEC model for January 2008 as an example. The main currents are the East Greenland Current (EGC), North Atlantic Current (NAC) and the Norwegian Coastal Current (NCC). Only one of each 25 vectors is drawn. LH, SF and SP denote La Hague, Sellafield and Springfields reprocessing plants.

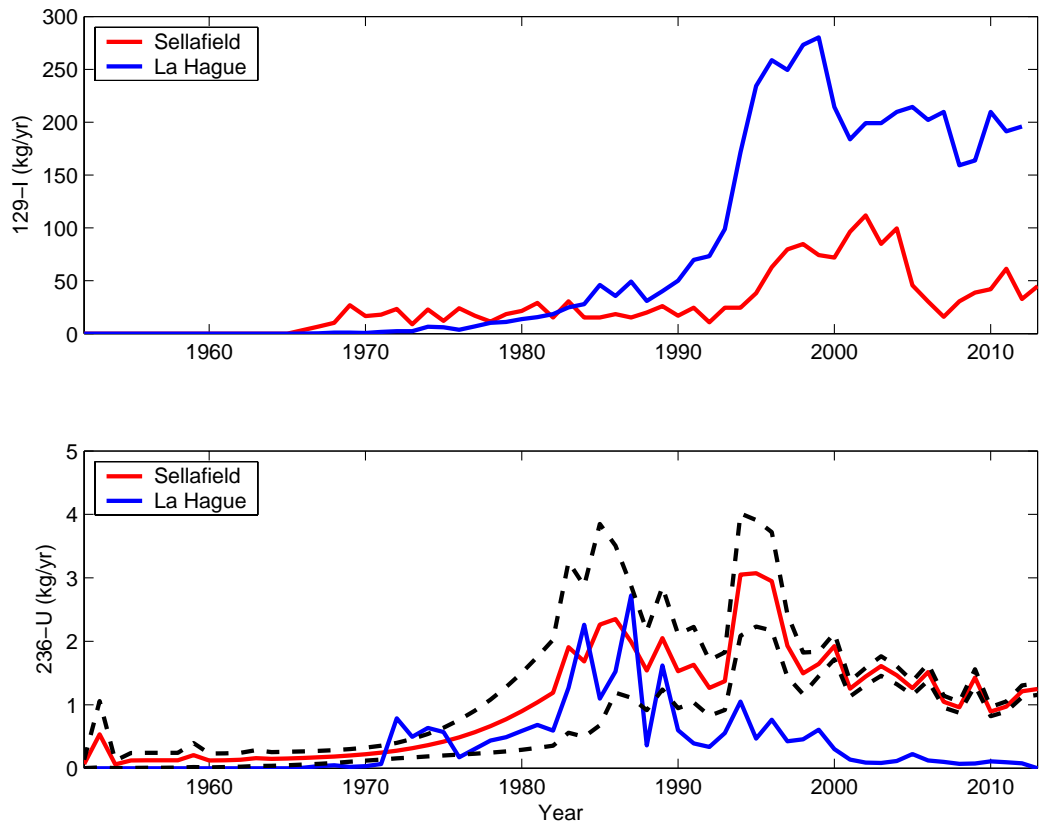


Figure 2: Annual releases of  $^{129}\text{I}$  and  $^{236}\text{U}$  from Sellafield and La Hague reprocessing plants. Dashed black lines indicate the lower and upper limits of the estimation of  $^{236}\text{U}$  releases from Sellafield.

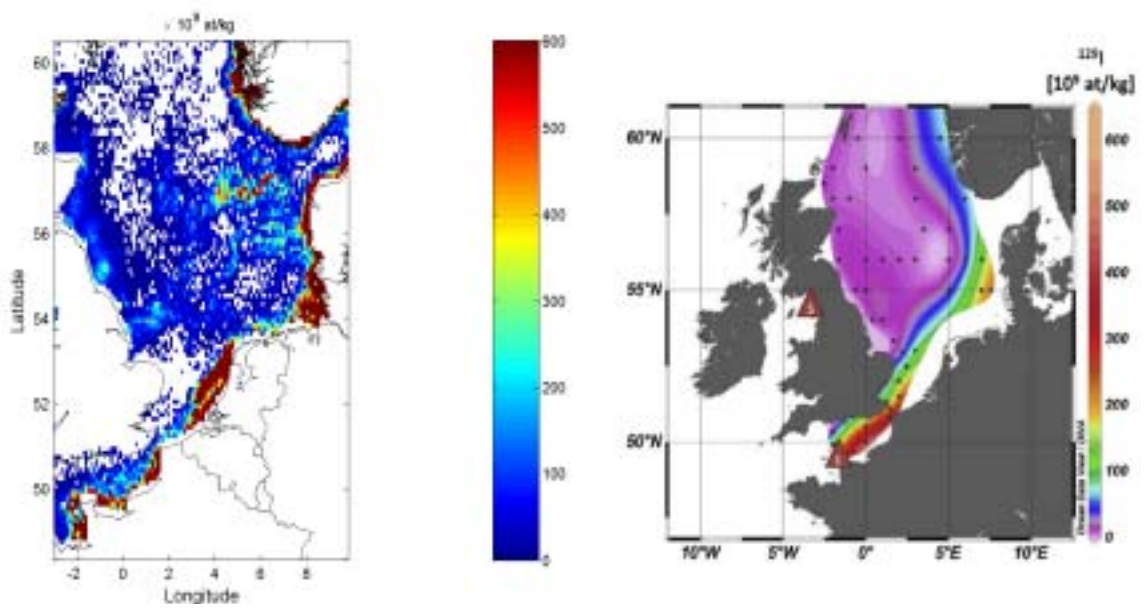


Figure 3: Calculated, left side, and measured, right side, (Christl et al., 2015b)  $^{129}\text{I}$  concentrations in surface water of the North Sea in 2009. White areas in the sea in the calculated map indicate regions with fallout background concentration.

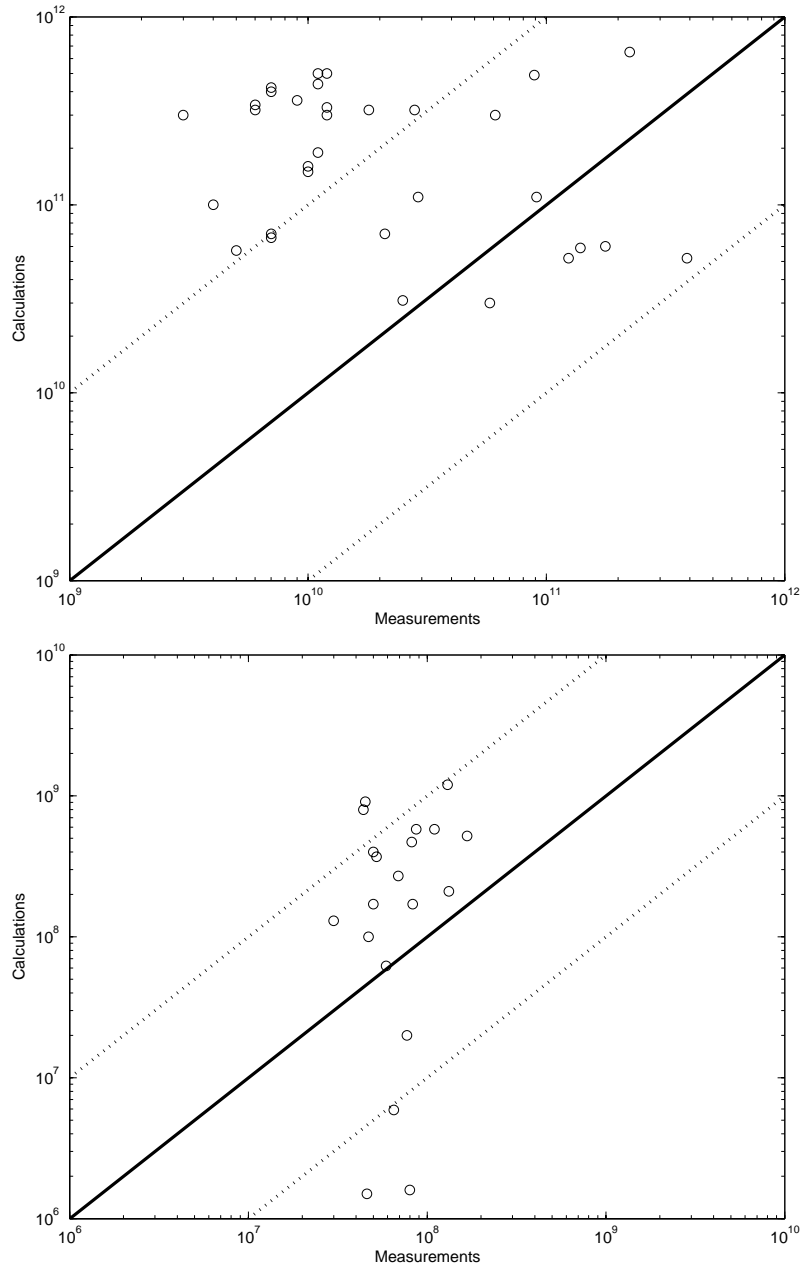


Figure 4: Calculated vs. measured concentrations (at/kg) in Christl et al. (2015b). Top and bottom panels:  $^{129}\text{I}$  and  $^{236}\text{U}$  respectively.

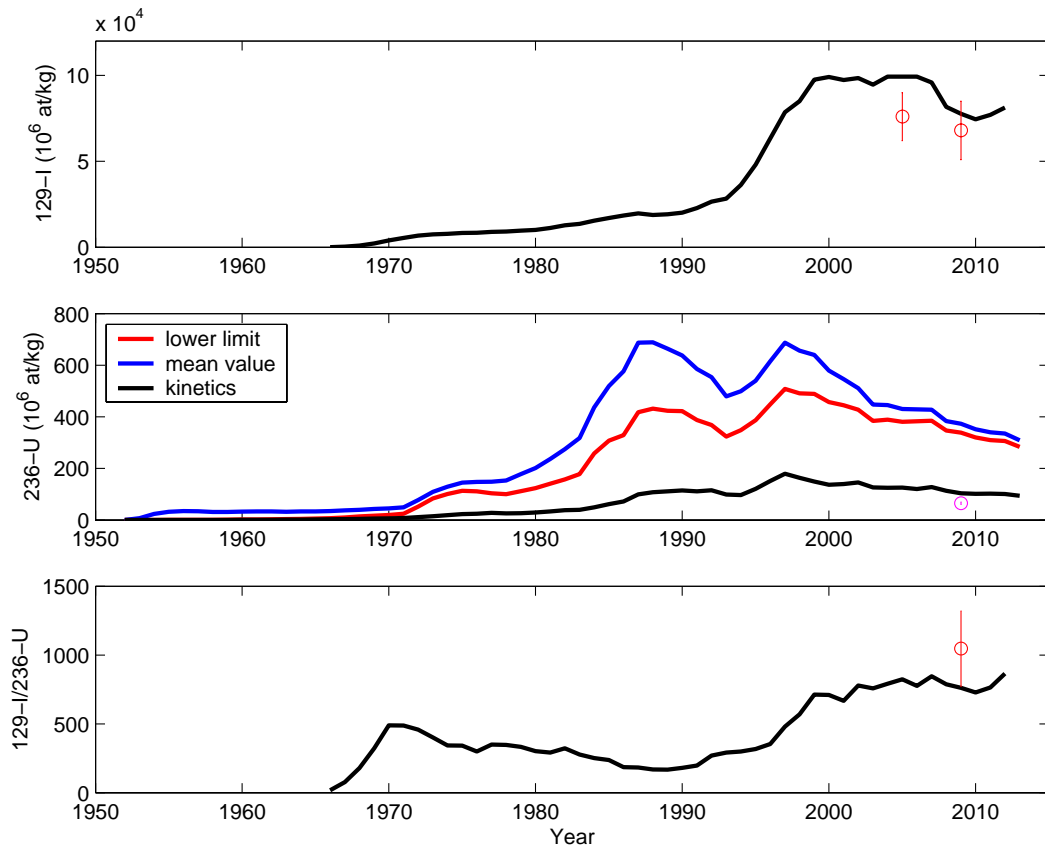


Figure 5: Top: calculated and measured mean  $^{129}\text{I}$  concentrations in surface water of the North Sea. Middle panel: the same but for  $^{236}\text{U}$ . See the text for explanation of the legend. Bottom: Calculated and measured mean  $^{129}\text{I}/^{236}\text{U}$  ratios in surface water of the North Sea.

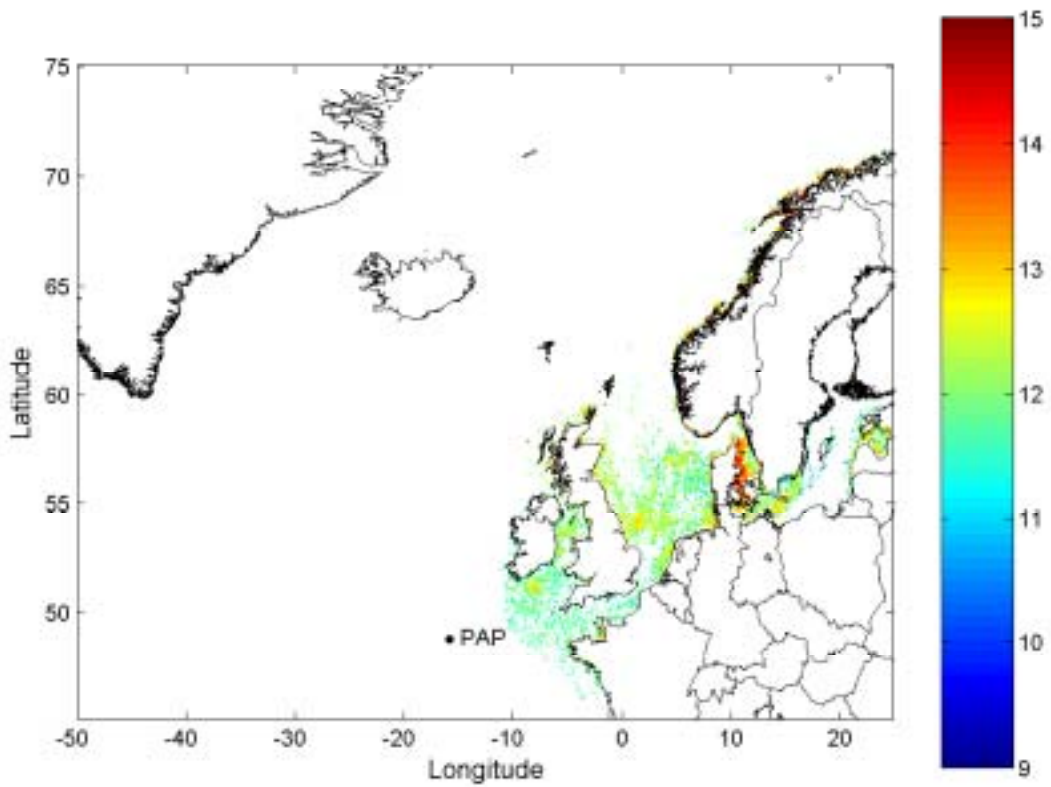


Figure 6: Calculated  $^{236}\text{U}$  inventory ( $\text{at}/\text{m}^2$ , logarithmic scale) in bed sediments of the model domain in 2013.



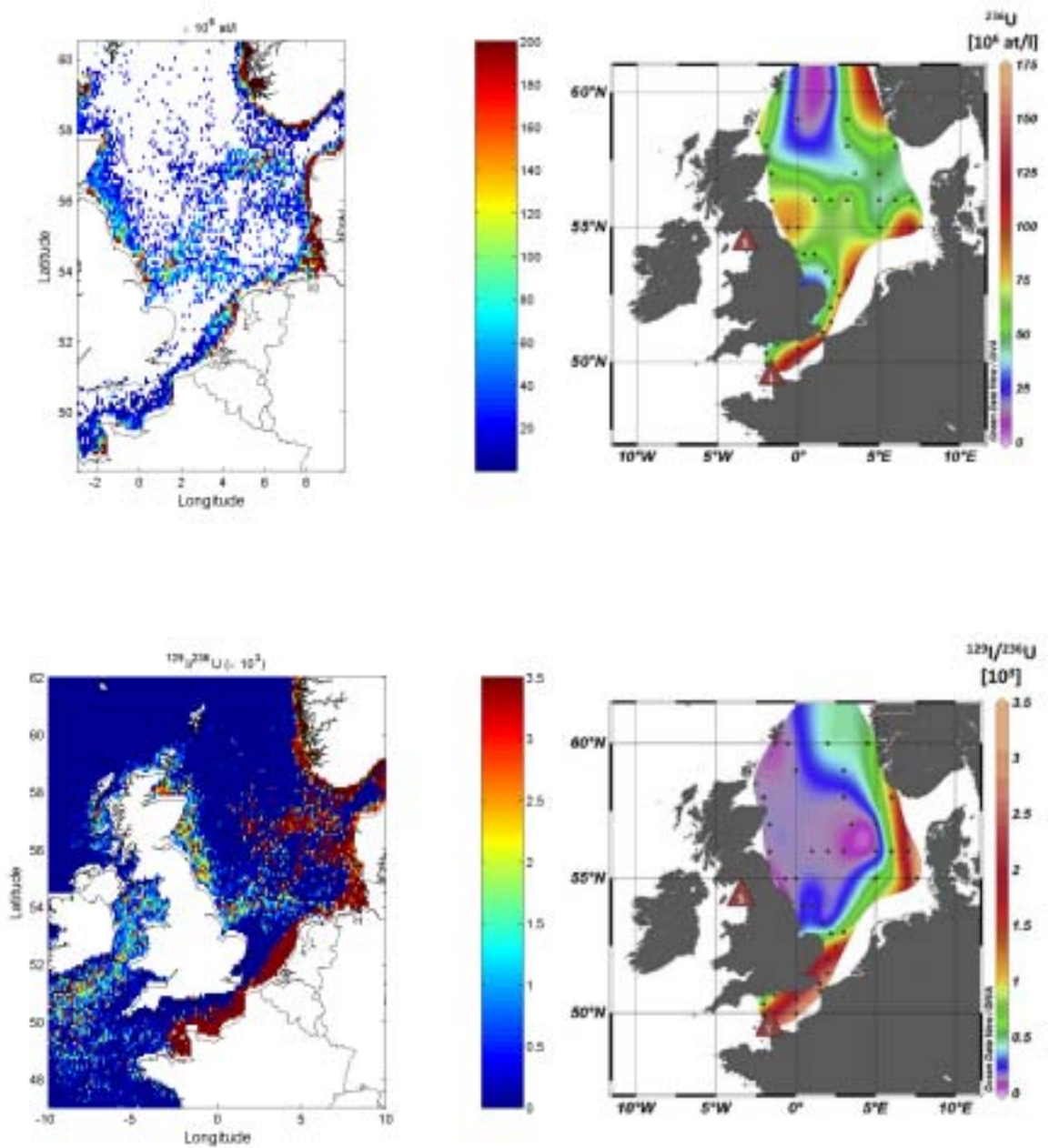


Figure 7: Calculated (left side) and measured (Christl et al., 2015b; right side)  $^{236}\text{U}$  concentrations in surface water of the North Sea in 2009 (top row). White areas in the sea in the calculated map indicate regions with fallout background concentration.  $^{129}\text{I}/^{236}\text{U}$  ratio in surface water (bottom row).

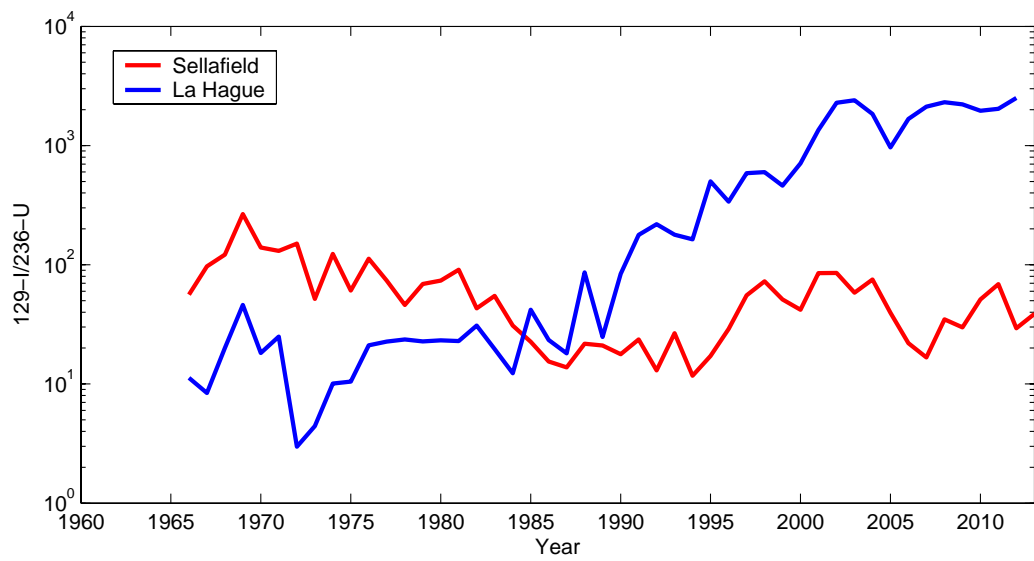


Figure 8: Annual  $^{129}\text{I}/^{236}\text{U}$  ratios in the releases from Sellafield (lower value of the estimation, which is used in the model) and La Hague reprocessing plants.

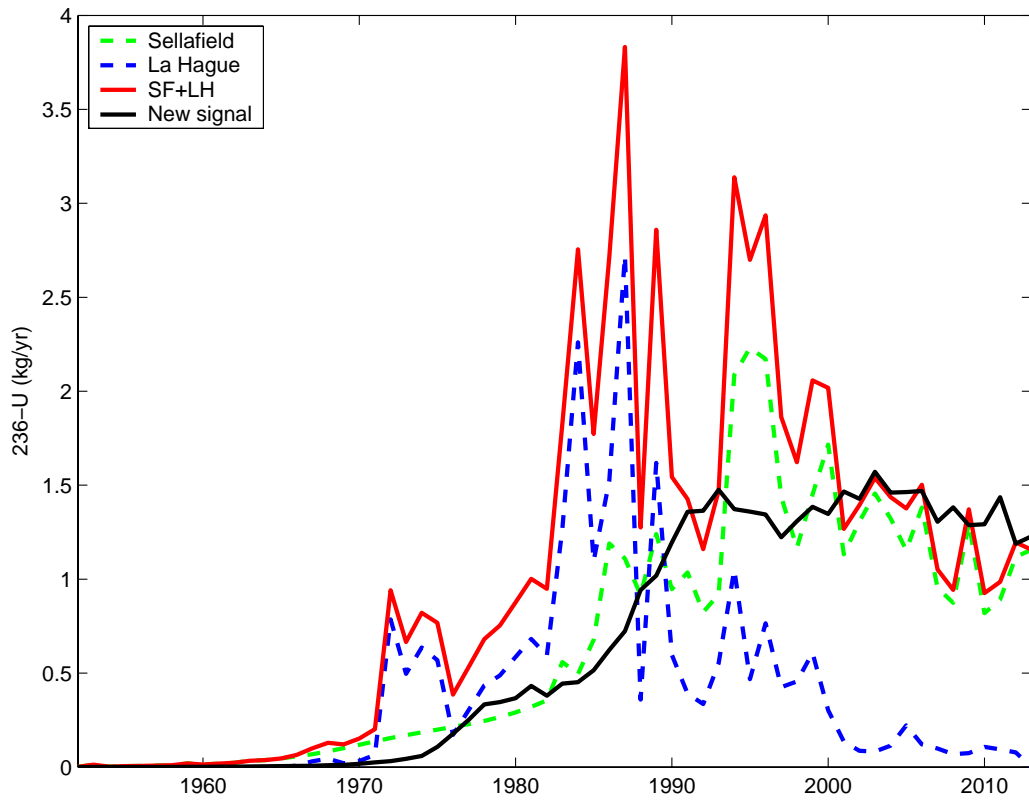


Figure 9: Annual  $^{236}\text{U}$  input into the Arctic (black line) together with the releases from Sellafield (green dashed line), La Hague (blue dashed line) and the sum of both (red solid line).